Carbon Nanoelectronics: Unzipping Tubes into Graphene Ribbons

H. Santos, L. Chico, and L. Brey

Instituto de Ciencia de Materiales de Madrid (CSIC), Cantoblanco, 28049 Madrid, Spain

(Received 23 April 2009; published 20 August 2009)

We report on the transport properties of novel carbon nanostructures made of partially unzipped carbon nanotubes, which can be regarded as a seamless junction of a tube and a nanoribbon. We find that graphene nanoribbons act at certain energy ranges as perfect valley filters for carbon nanotubes, with the maximum possible conductance. Our results show that a partially unzipped carbon nanotube is a magnetoresistive device, with a very large value of magnetoresistance. We explore the properties of several structures combining nanotubes and graphene nanoribbons, demonstrating that they behave as optimal contacts for each other, and opening a new route for the design of mixed graphene-nanotube devices.

DOI: 10.1103/PhysRevLett.103.086801 PACS numbers: 81.05.Uw, 73.20.−r

Introduction.—The experimental isolation of graphene [1] and the anomalous electronic properties of its carriers [2,3] have rapidly motivated intense theoretical and experimental investigation, among many other characteristics, of its transport properties [4]. The valence and conduction bands of graphene touch at two inequivalent points of the Brillouin zone. Near these points, the dispersion relation is linear, so graphene carriers behave as massless Dirac fermions. The large separation in reciprocal space of the Dirac points suppress intervalley scattering in pure graphene samples [5]. Thus, besides the spin and charge degree of freedom, graphene carriers should be also characterized by a valley index [4,6].

Because of its two-dimensional character, graphene can be patterned using high-resolution lithography [7], so in principle nanocircuits with transistors and interconnects can be fabricated in the same graphene layer in a fully compatible way with the present electronic technology. In these nanodevices, graphene nanoribbons could be used as connectors [8]. Lithographic techniques have been employed to produce wide (> 20 nm) stripes of graphene [9,10], but with limited smoothness due to limitations in the resolution. Chemical [11,12] and synthetic [13] methods have been employed successfully, albeit producing microscopic quantities of graphene nanoribbons. Bulk production of ribbons has been achieved with a chemical vapor deposition method, but the samples had a wide dispersion in size and number of layers [14], so the controlled fabrication of nanoribbons of small width remained as a technological challenge.

Quite recently, three experimental groups announced simultaneously a promising way to fabricate narrow graphene nanoribbons (GNR) using carbon nanotubes as starting material [15–17]. These three groups propose to longitudinally unzip carbon nanotubes (CNTs) to make nanoribbons, either by chemical attack [15], by plasma etching [16], or by lithium intercalation followed by exfoliation [17], with very high yields. Unzipping carbon nanotubes appears as a promising way to fabricate narrow nanoribbons needed for nanoelectronic applications.

In this Letter, we report on the electronic transport properties of unzipped carbon nanotubes. We propose that partial unzipping of carbon nanotubes can actually be used to produce a new class of carbon-based nanostructures, which combine nanoribbons and nanotubes. By studying the GNR/CNT junction, we conclude that nanoribbons and nanotubes behave as ideal contacts for each other. Furthermore, we obtain that structures formed by zigzag-terminated GNR and armchair CNT units behave as spin and valley filters, and can be used as building blocks for carbon-based devices featuring very large magnetoresistance.

Ingredients.—(i) Carbon nanotubes are rolled-up cylinders of graphene [18]. Their electronic properties can be approximately derived from the graphene band structure by imposing the Born–von Kármán boundary condition [19], and depending on their geometry, can behave as metals or semiconductors [20,21]. In this work, we focus in armchair carbon nanotubes [19]; they are denoted by (n, n), being $2n$ the number of carbon atoms at the CNT circumference. Armchair nanotubes are one-dimensional metals with two inequivalent Fermi points in the Brillouin zone, reminiscent of the graphene Dirac points.

(ii) Carbon nanoribbons are obtained by cutting graphene in the form of a quasi-one-dimensional stripe. The electronic properties of GNR strongly depend on the atomic edge termination. There are two basic shapes for graphene edges, armchair and zigzag [22]. The GNR electronic properties can be derived from the graphene band structure by imposing the appropriate boundary conditions [23]. Armchair GNR can be either metallic or semiconducting depending on their width, whereas for the zigzag GNR (ZGNR), twofold degenerated flat bands lie at the Fermi energy. These bands are associated with edge states [23] and their dispersionless character favors an insulating antiferromagnetic ground state, with opposite magnetization at the edges [22,24–27]. Zigzag graphene nanoribbons are obtained by unrolling an armchair CNT, see Fig. 1. The ZGNR width is defined by the number n of zigzag rows in the unit cell; the usual notation for such ribbon is n-ZGNR.

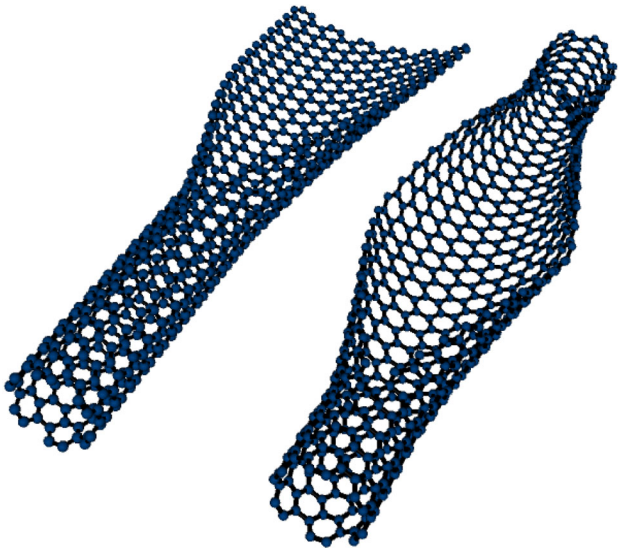

FIG. 1 (color online). Geometry of two partially unzipped nanotubes. Left: a (6,6) armchair nanotube unzipped into a 12-ZGNR, making a CNT/GNR single junction. Right: the same nanotube unzipped in its central part, yielding a zigzag nanoribbon quantum dot connected to armchair nanotube contacts.

In this work, we study partially unzipped carbon nanotubes, such as those shown in Fig. 1, which are equivalent to a combination of carbon nanotubes and graphene nanoribbons. In what follows, we focus in armchair carbon nanotubes and the derived ZGNR.

Model Hamiltonian and transport calculation.—We describe the motion of carriers between π orbitals with a first-neighbor hopping t. The electronic repulsion is included within the Hubbard model, which we solve at the mean-field level. For $t = 2.66$ eV and the Hubbard term in the range $1.5\ \text{eV} < U < 3\ \text{eV}$, this approach describes adequately the main features of the *ab initio* calculations [24,28] of GNR. The Hamiltonian reads

$$H = -t\sum_{i,j,\sigma} c^{\dagger}_{i,\sigma}c_{j,\sigma} + U\sum_{i,\sigma} n_{i,\sigma}\langle n_{i,-\sigma}\rangle, \qquad (1)$$

where $c^{\dagger}_{i,\sigma}$ is a creation operator at atom i of a π electron with spin σ. We consider that the effect of the unzipping is to cut the hopping between the carbon atoms where the opening occurs, and we assume that unzipping does not modify the hopping between the other carbon atoms. This Hamiltonian depends on the electronic occupation and is solved self-consistently [29].

As the systems lack translational invariance, we follow a Green function (GF) approach to calculate the electronic and transport properties [30,31]. To this purpose, we divide the system into three parts, namely, a central region connected to the right and left leads. The Hamiltonian can thus be written as

$$H = H_C + H_R + H_L + h_{LC} + h_{RC}, \qquad (2)$$

where H_C, H_L, and H_R are the Hamiltonians of the central portion, left and right leads, respectively, and h_{LC}, h_{RC} are the hoppings from the left L and right R lead to the central region C. The GF of the latter is

$$\mathcal{G}_C(E) = (E - H_C - \Sigma_L - \Sigma_R)^{-1}, \qquad (3)$$

where $\Sigma_\ell = h_{\ell C} g_\ell h^{\dagger}_{\ell C}$ is the self-energy due to lead $\ell = L$, R, and $g_\ell = (E - H_\ell)^{-1}$ is the GF of lead ℓ.

In a zero bias approximation, the Landauer conductance G is given by $G = \frac{2e^2}{h}\mathcal{T}(E_F)$. $\mathcal{T}$ is the transmission function, that can be obtained from the GFs of the central part and the leads:

$$\mathcal{T}(E) = \mathrm{Tr}[\Gamma_L(E)\mathcal{G}_C(E)\Gamma_R(E)\mathcal{G}^{\dagger}_C(E)], \qquad (4)$$

where $\Gamma_\ell = i(\Sigma_\ell - \Sigma^{\dagger}_\ell)$ describes the coupling of the central region C to lead ℓ. For a single junction, the left and right electrodes are connected directly, so $\mathcal{G}_C$ in Eq. (4) is just the GF of the interface between the left and right lead, $\mathcal{G}_{LR}$.

Results.—In Fig. 2, we show the conductance of a single (6,6) CNT/12-ZGNR junction, as the one depicted in the upper panel of Fig. 1, for noninteracting electrons ($U = 0$). As a reference, we show in dashed and dotted lines the conductances of the perfect infinite CNT and ZGNR. Around zero energy, the conductance of the junction is equal to that of the perfect nanoribbon, demonstrating that the (6,6) CNT acts as a transparent contact for the 12-ZGNR. Assuming left to right conduction, the ZGNR only has the K' channel open to transport, and it is completely transparent to states from the corresponding K' valley of the CNT. This indicates that backscattering is practically zero in the device and the conductance in this energy range is set by the ribbon, which acts as a valley

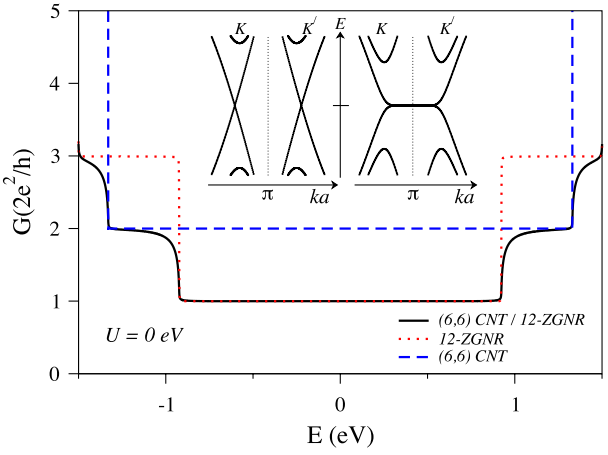

FIG. 2 (color online). Solid line: conductance of a (6,6) CNT/12-ZGNR junction. Dashed (dotted) line: conductance of a perfect infinite (6,6) CNT (12-ZGNR). The results correspond to $U = 0$. The insets show the band structures of the armchair nanotube (left) and the zigzag nanoribbon (right). The flat bands joining the Dirac points in the ZGNR corresponds to states localized at the edges of the ribbon.

filter for the CNT. Our numerical results show that states from the K valley of the CNT cannot transverse the junction. At higher energies, more channels open in the ribbon, so the conductance now is limited by that of the (6,6) nanotube: here, the ribbon is acting as a transparent contact for the CNT, and transport from both valleys is allowed. Calculations with larger systems, such as an (18,18) CNT/36-ZGNR (not shown here) yield similar results, with the obvious increase in the number of channels. We have also investigated the narrowing of the ribbon part, such as a (6,6) CNT/10-ZGNR, or an (18,18) CNT/32-ZGNR, finding that the effect is robust against the precise form of the CNT/ZGNR junction.

As discussed above, the interaction between electrons changes dramatically the band structure of graphene nanoribbons near the Fermi energy. In the following, we analyze how the interactions modify the low energy transport properties. Figure 3 shows the effect of electron-electron interactions in the conductance of the (6,6) CNT/12-ZGNR junction for $U = 2$ eV and $U = 3$ eV. The inset shows the band structure for the (6,6) CNT and for the 12-ZGNR for an interaction $U = 3$ eV. For CNTs, the Hubbard interaction does not modify the magnetic moments on the carbon atoms, so the effect of U is just a rigid shift of the electronic structure. In the case of ZGNR, the interaction orders ferromagnetically the most external atoms at each edge, and the magnetic moments on opposite edges couple antiferromagnetically. Magnetic order induces dispersion of the edge bands along the edge direction, opening a gap at the center of the band structure that increases with the value of the interaction U. The states with opposite spin orientation are degenerated, but the edge bands with opposite spin correspond to states located at opposite edges. The many body-induced gap in ZGNR precludes transport near the Fermi energy. Above the gap, there is a region of enhanced conductance with respect to the noninteracting case. This occurs because the dispersion of the edge states, induced by the electron-electron interaction, opens a new electronic channel near each Dirac point of the ZGNR, as, for example, at point C in the inset of Fig. 3. Besides transmission from K' to K' valleys observed in the noninteracting case, now a state A in the CNT K valley can be transmitted into state C of the ZGNR at the same valley, giving an enhanced conductance. The width of this bump in the conductance is proportional to the midband gap and increases with U. The state C is a edge state, and for opposite spin orientations, the wave function of this state is localized in opposite edges. Therefore, the excess of current with respect to the noninteracting case (bump regions of Fig. 3) is localized at the edges and with opposite spin polarization. Above this energy region, there is an energy interval where the conductance gets the value $2e^2/h$, and valley filtering occurs, as explained for the noninteracting case. This energy interval is around 0.6 eV for $U = 2$ eV, making it possible the observation of this filtering in carbon nanotubes. Above this interval, the conductance values are quite similar to the noninteracting cases, demonstrating the high transparency of armchair CNTs for ZGNR and vice versa.

The application of a magnetic field, B, changes dramatically the electronic structure of the nanoribbon. The Zeeman coupling between the electron spin and B competes with the antiferromagnetic coupling between the nanoribbon edges, and for large enough B, the Zeeman interaction favors ferromagnetic order. The ferromagnetic solution is obtained by solving self-consistently Hamiltonian, Eq. (1), with a ferromagnetic initial guess. In the left inset of Fig. 4, we plot the band structure of a ZGNR in the ferromagnetic configuration. In this arrangement, the energy of the spin up and spin down edge

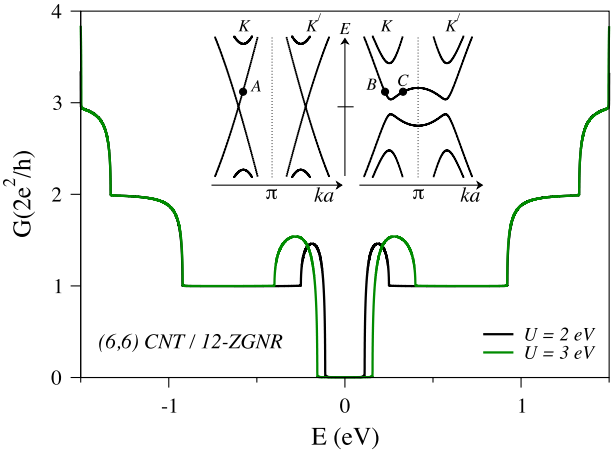

FIG. 3 (color online). Conductance of a (6,6) CNT/12 ZGNR with on-site repulsion ($U = 2$ and 3 eV). Insets show the band structures of the armchair nanotube (left) and the zigzag nanoribbon (right) for $U = 3$ eV.

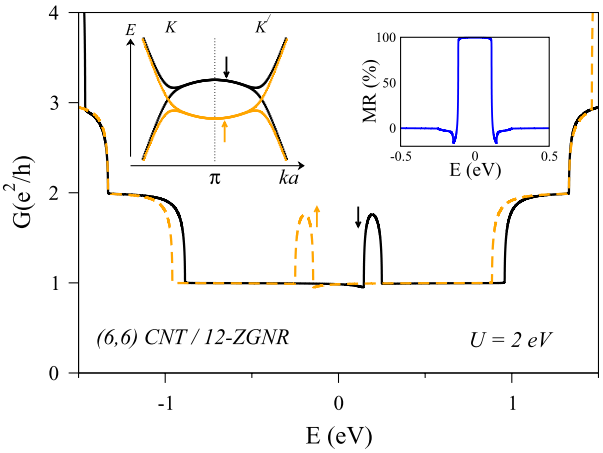

FIG. 4 (color online). Conductance of a (6,6) CNT/12 ZGNR in the ferromagnetic configuration. Left inset shows the band structure of the ZGNR. Dark (light) lines correspond to electron spin orientation parallel (antiparallel) to the magnetic field. Right inset shows the magnetoresistance of the device as function of energy.

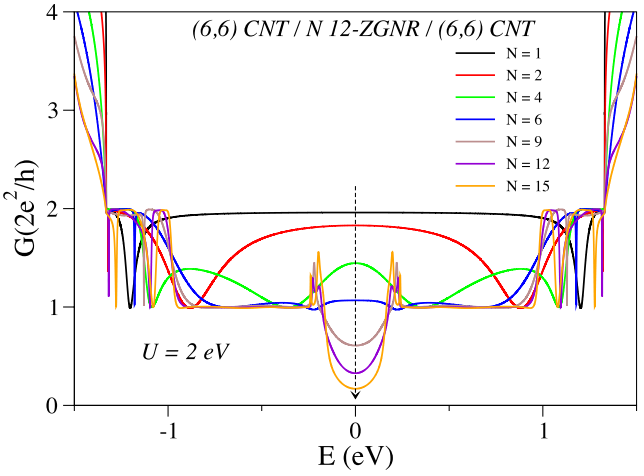

FIG. 5 (color online). Conductance of a (6,6) CNT/N12-ZGNR/(6,6) CNT with on-site repulsion $U = 2$ eV for several ribbon lengths ($N = 1$ to $N = 15$). The arrow indicates increasing system size.

localized states splits, and because of electron hole symmetry, they cross at zero energy. Therefore, a magnetic field makes the ZGNR ferromagnetic and metallic. The magnetic field closes the midgap of the antiferromagnetic configuration, opening new transport channels at low energies. This generates a finite value of the conductance near the Fermi energy, where the antiferromagnetic solution was insulating, see Fig. 4. Therefore, B produces a dramatic change in the conductance of the system, which is quantified by the magnetoresistance, defined as the relative change of the resistance when an applied magnetic is applied. The results in the right inset of Fig. 4 indicate a magnetoresistance close to 100% near the Fermi energy. The B for switching the order of the ZGNR from antiferromagnetic to ferromagnetic depends on U, the length and width of the ribbon and the temperature. In Ref. [27], it has been estimated that the switching B can be as low as 0.03 T for 4 K. We propose that a single unzipped carbon nanotube is by itself a device featuring 100% magnetoresistance.

We have also explored the properties of double junction systems, such as the one depicted in Fig. 1 (right), an infinite armchair (6,6) nanotube open in its central part making a ZGNR. We denote this structure as (6,6) CNT/N 12-ZGNR/(6,6) CNT, where N is the number of unit cells in the nanoribbon. The transparency of the nanotube contacts is evident in Fig. 5: the transmission through the central ribbon part is higher than in an infinite ribbon for the smaller sizes, and slowly decays to the zero limit value in the gap with increasing ribbon size. Other combinations, such a CNT quantum dot with ribbon contacts, can be envisioned, expanding the possibilities of carbon electronics, in analogy to the quantum dot and superlattice structures proposed for CNTs [32,33].

In summary, we propose a new class of carbon nanostructures based on unzipped nanotubes, which actually consist of mixed carbon nanotube-nanoribbon systems. We have found that ribbons from unzipped tubes behave as completely transparent contacts for the parent tubes, and vice versa. Our results demonstrate that partially unzipped carbon nanotubes are by themselves magnetoresistive devices, with a large value of the magnetoresistance. Furthermore, carbon nanoribbons act as valley filters for carbon nanotubes; this behavior is robust with respect to the inclusion of electron-electron interaction, opening the possibility of exploiting the valley degree of freedom in a new class of carbon-based nanodevices.

This work has been partially supported by the Spanish DGES under Grants No. MAT2006-06242 and No. MAT2006-03741 and Spanish CSIC under Grant No. PI 200860I048.

[1] K. S. Novoselov *et al.*, Science **306**, 666 (2004).
[2] K. S. Novoselov *et al.*, Nature (London) **438**, 197 (2005).
[3] Y. Zhang *et al.*, Nature (London) **438**, 201 (2005).
[4] A. H. Castro-Neto *et al.*, Rev. Mod. Phys. **81**, 109 (2009).
[5] A. F. Morpurgo *et al.*, Phys. Rev. Lett. **97**, 196804 (2006).
[6] A. Rycerz *et al.*, Nature Phys. **3**, 172 (2007).
[7] C. Berger *et al.*, Science **312**, 1191 (2006).
[8] A. Iyengar *et al.*, Phys. Rev. B **78**, 235411 (2008).
[9] M. Y. Han *et al.*, Phys. Rev. Lett. **98**, 206805 (2007).
[10] B. Özyilmaz *et al.*, Phys. Rev. Lett. **99**, 166804 (2007).
[11] H. C. Schniepp *et al.*, J. Phys. Chem. B **110**, 8535 (2006).
[12] X. Li *et al.*, Science **319**, 1229 (2008).
[13] X. Yang *et al.*, J. Am. Chem. Soc. **130**, 4216 (2008).
[14] J. Campos-Delgado *et al.*, Nano Lett. **8**, 2773 (2008).
[15] D. V. Kosynkin *et al.*, Nature (London) **458**, 872 (2009).
[16] L. Jiao *et al.*, Nature (London) **458**, 877 (2009).
[17] A. G. Cano-Márquez *et al.*, Nano Lett. **9**, 1527 (2009).
[18] S. Iijima, Nature (London) **354**, 56 (1991).
[19] R. Saito *et al.*, *Physical Properties of Carbon Nanotubes* (Imperial College, London, 1998).
[20] N. Hamada *et al.*, Phys. Rev. Lett. **68**, 1579 (1992).
[21] M. Dresselhaus, Physics World **9**, 18 (1996).
[22] M. Fujita *et al.*, J. Phys. Soc. Jpn. **65**, 1920 (1996).
[23] L. Brey and H. A. Fertig, Phys. Rev. B **73**, 235411 (2006).
[24] J. Fernández-Rossier, Phys. Rev. B **77**, 075430 (2008).
[25] Y. Son *et al.*, Phys. Rev. Lett. **97**, 216803 (2006).
[26] L. Pisani *et al.*, Phys. Rev. B **75**, 064418 (2007).
[27] F. Muñoz-Rojas *et al.*, Phys. Rev. Lett. **102**, 136810 (2009).
[28] J. Fernández-Rossier *et al.*, Phys. Rev. Lett. **99**, 177204 (2007).
[29] M. P. López Sancho *et al.*, Phys. Rev. B **63**, 165419 (2001).
[30] L. Chico *et al.*, Phys. Rev. B **54**, 2600 (1996).
[31] M. B. Nardelli, Phys. Rev. B **60**, 7828 (1999).
[32] L. Chico *et al.*, Phys. Rev. Lett. **81**, 1278 (1998).
[33] W. Jaskólski *et al.*, Phys. Rev. B **71**, 155405 (2005).